Structural Analysis of Historical Constructions, New Delhi 2006
P.B. Lourenço, P. Roca, C. Modena, S. Agrawal (Eds.)

Experimental and Analytical Out-of-Plane Behaviour of Calcarenite Masonry Walls

Liborio Cavaleri, Marinella Fossetti, Lidia La Mendola and Maurizio Papia
University of Palermo, Dipartimento di Ingegneria Strutturale e Geotecnica, Italy

ABSTRACT: In the paper a procedure for the prediction of the response of masonry walls under lateral forces orthogonal to the middle plane in the case of one dimensional behaviour, based on the hypothesis of plane cross-section and a nonlinear σ–ε equivalent law for the material is presented. The proposed procedure is supported by an experimental investigation involving calcarenite masonry walls. The characteristics of the above procedure are discussed and the strategy to improve the obtainable analytical results is suggested for the analysis of the types of walls investigated.

1 INTRODUCTION AND STATEMENT OF THE PROBLEM

In masonry buildings vertical loads are often transmitted to the walls eccentrically. Further, due to thrusting elements (roof, arches, etc) and seismic events, horizontal loads orthogonal to the middle plane also rise. In these conditions the flexural capacity of the masonry is involved.
In several ancient masonry structures, because of the low level of the constraints with the orthogonal walls or because of the high ratio between the wall height and the distance between the lateral constraints, bearing walls can be considered as one-dimensional vertical elements (Fig.1). The response of these elements can be predicted if the moment-curvature law of the cross-sections is available.

Referring to the problem of the identification of the masonry cross-section behaviour few studies can be found in the literature which are mainly based on the linear behaviour of the material in compression and on its no tensile strength (e.g. Yokel 1971, Schulz et al. 2001, Drysdale and Hamid 1983, Hatzinikolas et al. 1980, Cantù 1982). Nevertheless some studies, in which the tensile strength of the material is considered, have been done (e.g. Lu et al. 2004).

The mechanical nonlinear behaviour of the material is often not considered for sake of simplicity or because of the prevalence of the second order effects on the mechanical nonlinearity. This prevalence is stronger as much slenderer the considered elements are. Note, however, that also in the case of slender elements a correct evaluation of the critical state should be based on the real mechanical behaviour of the material, because its non-linearity may lead to results quite different from the ones based on the assumption of linear behaviour, as proved by La Mendola (1997) and by Lu et al. (2004).

Referring to the materials studied by the scientific community, by analyzing the specialist literature one finds that masonry elements made of clay blocks (or bricks) and mortar or concrete blocks and mortar are mainly investigated (e.g. Crook 1982, Macchi 1982, AlShebani and Sinha 2000, Griffith et al. 2004, Hansen 2001), while very few works deal with calcarenite block masonry.

Calcarenite is a limestone composed predominantly of clastic sand-size grains of calcite, or rarely aragonic, usually as fragments of shells or fossils. It represents the most diffused material for masonry in the countries of the Mediterranean area and it is also diffused as construction

material in Portugal, France, England, U.S., Mexico, South America, etc. It was especially used in the past as many historical constructions evidence.

Missing specialist investigations, this work may constitute a contribution to the study of the flexural nonlinear behaviour of calcarenite masonry walls.

A special study has already been done by the authors of this paper (Cavaleri et al. 2005) and supported by an experimental investigation; it shows a procedure for the determination of a nonlinear moment-curvature law of masonry cross-sections basing on the definition of a general stress-strain law in compression for the material (La Mendola and Papia 2002, Sargin 1971).

The present work is an extension of the above study and it is addressed to the prediction of the response of bearing walls subjected to lateral loads: how a model for a masonry wall can be defined is shown taking the mean nonlinear characteristics of the material into account. An experimental investigation is coupled to an analytical one, in order to observe the behaviour of full scale walls under compressive loads and horizontal loads orthogonal to the middle plane, and in order to test the reliability of the model before mentioned.

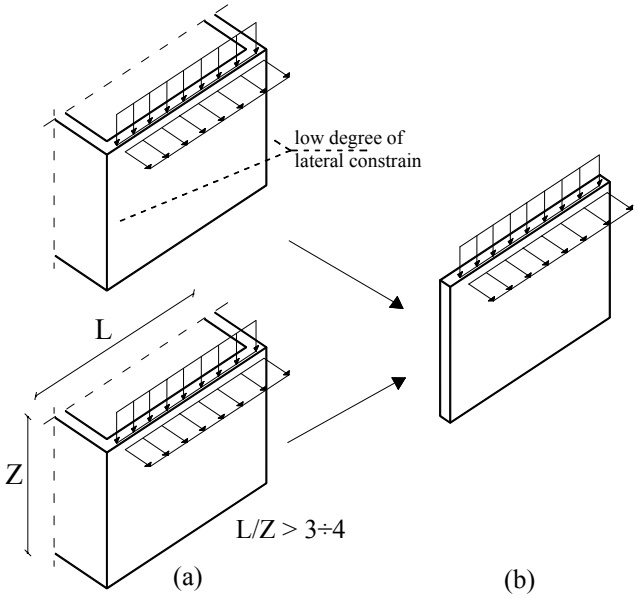

Figure 1: Examples of three-dimensional (a) and equivalent plane (b) schemes for analysis of walls.

The experimental tests allowed to clarify the effects of the nonlinear behaviour of the material and the effects of the slenderness on the global response of walls in connection with the kind of the masonry considered.

2 CONSTITUTIVE LAW FOR THE MATERIAL

In order to model the behaviour of the masonry in compression the masonry itself was considered as a continuum homogeneous governed by a constitutive conventional law σ–ε. This approach is different from the techniques based on the definition of a constitutive law for the components (mortar and blocks) and a constitutive law for the interface between them. Moreover it simplifies very much the problem of the mechanical characterization of the material.

Samples of the material constituted by three rows of calcarenite blocks were tested in compression giving an experimental global σ–ε response. It was shown that this response can be fitted by the analytical law given by Sargin (1971) for concrete, that is

$$\widetilde{\sigma} = \frac{A\widetilde{\varepsilon} + (D-1)\widetilde{\varepsilon}^2}{1 + (A-2)\widetilde{\varepsilon} + D\widetilde{\varepsilon}^2}, \quad \widetilde{\varepsilon} = \frac{\varepsilon}{\varepsilon_0}, \quad \widetilde{\sigma} = \frac{\sigma}{\sigma_0} \tag{1}$$

where A and D are parameters to be calibrated by experimental tests while σ_0 is the maximum compression stress and ε_0 is the corresponding strain.

With variation in A and D many types of materials can be modelled. Generally, for masonry, A has to be chosen in the range 2÷3 while D has to be chosen in the range 0÷2x(A-1). For the case examined, 2.8 and 1.5 are the values chosen respectively for A and D, these values giving a good accordance with the experimental data.

The complete definition of the σ–ε law for the material requests to fix appropriate values for the peak of resistance σ_0 and the corresponding strain ε_0. These values were fixed by examining the experimental results: 1.3 mm/m was chosen for ε_0 and 4 MPa for σ_0.

In Fig. 2-a a good agreement can be observed between the experimental results obtained from 6 samples and the analytical law proposed by Sargin in which the value of A and D were assigned as above.

The σ–ε law for the masonry can be used for the analysis of cross-sections under bending moment and centred compressive load. Solving the problem of evaluating the distribution of the stresses in a generic cross-section requires the definition of the strain distribution. In the most simplified case the strain distribution is considered linear, that is to say the generic cross-section remains plane. This hypothesis makes it sufficiently simple to evaluate the limit condition of the cross-section in the case of nonlinear mechanical behaviour of the material. Nevertheless, the above hypothesis must be verified.

Proper tests under eccentric loads had the aim of proving the reliability of the hypothesis of plane cross-sections. A comparison between analytical and the experimental results obtained for some samples of masonry constituted by three rows of calcarenite blocks under an increasing vertical load with constant eccentricity e is inserted in Fig.2-b showing a good agreement as a proof of the effectiveness of the hypothesis of plane cross-section.

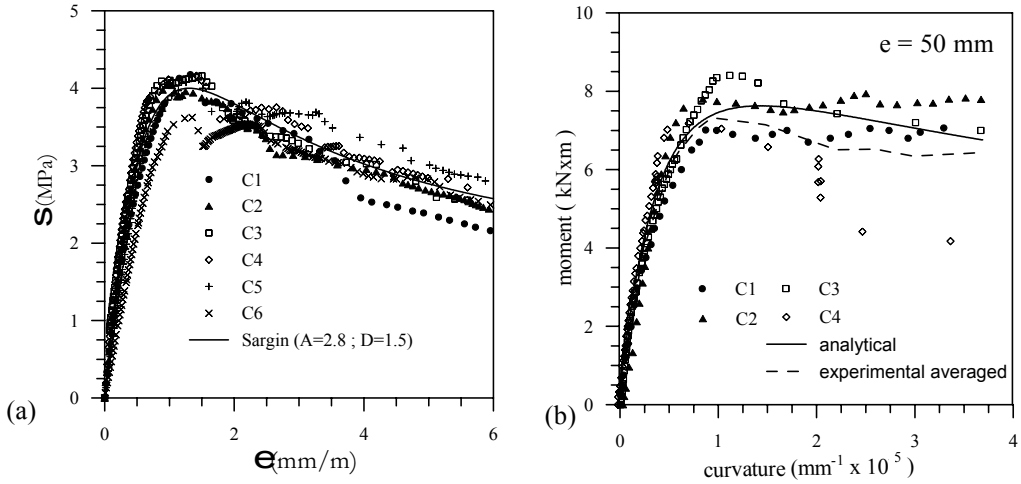

Figure 2 : Experimental and analytical stress-strain curves (a) and moment-curvature curves (b).

Much more details on this stage of the research are inserted in La Mendola and Papia 2002 and in Cavaleri et al. 2005.

3 EXPERIMENTAL INVESTIGATION

3.1 Test specimen and test set up

The specimens are walls of dimensions 740x210x2100 mm, made of calcarenite blocks and horizontal and vertical mortar joints. During each test the specimen was supported at the base by a trolley connected to a screw jack able to apply a controlled horizontal displacement and, at the top, it was constrained by an unmovable cylindrical hinge transmitting a vertical load by means of an hydraulic jack (Fig.3-a/b).

In these conditions the test device reproduces the schemes in Fig. 3-c, namely a cantilever wall subjected to a concentrated force orthogonal to the middle plane acting at the top contemporary to a vertical compressive load or alternatively a twice high wall subjected to a concentrated load orthogonal to the middle plane acting at the half height.

The tests were carried out by applying first the vertical load and then a monotonically increasing history of horizontal displacements at the base, maintaining constant the value of the vertical load. Hence every cross-section of the wall was subjected to an axial force and a bending moment.

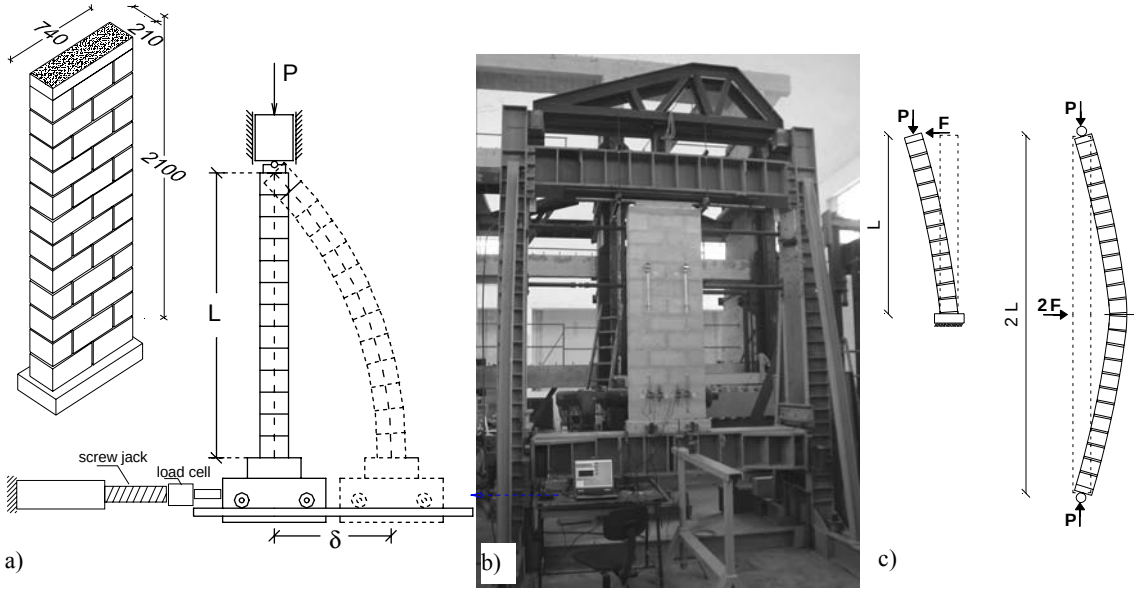

Figure 3 : Test specimen (a), test device (b) and equivalent loading schemes (c).

During the tests the reacting horizontal force at the base of the wall corresponding to the applied displacement was measured by means of a load cell. Further the vertical strains at the base of the wall were measured by 8 displacement transducers applied on the two sides of the wall, having different gauge lengths: four displacement transducers were inserted for each side at the base of the wall, two of them for measuring the strains between the first row of blocks and the third row of blocks including two horizontal joints (Fig. 4) and two for measuring the strains in the mortar joint nearest to the base joint.

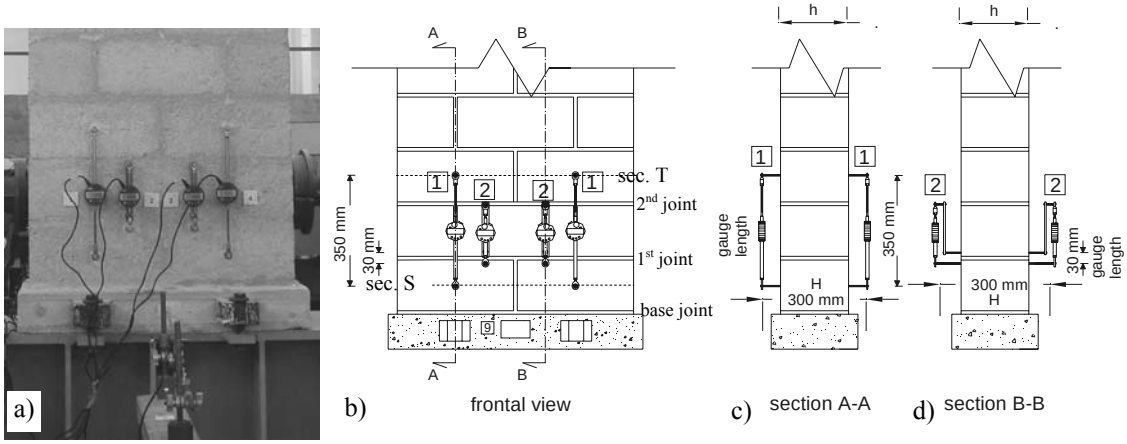

Figure 4 : Displacement transducers at the wall base: frontal view (a and b); lateral view (c and d).

By means of these measures the curvatures of the wall between two cross-sections including the first and the second joint were evaluated; further the curvatures that interested the joint nearest to the base one were evaluated. Observe that in the analyzed scheme the cross-sections near to the base are interested by the highest level of the bending moment and for this reason it was chosen to measure the curvatures there. The above measures allowed to know where the curvatures were higher (in the joints or in the calcarenite blocks) and the local response in terms of moment and corresponding curvature.

Four further displacement transducers (two for each side) were used before the horizontal displacements were applied in order to evaluate the elastic modulus of the masonry exhibited under the vertical load (see Fig. 3-b). In this way a comparison was made between the elastic characteristics of the material obtained by the masonry samples used for the determination of the σ–ε law, discussed in the previous section, and the elastic characteristics of the masonry of the walls.

Four specimens were tested: two of them monotonically up to the collapse (labelled W1 and W2) and the further two up to a limited horizontal force (labelled W3 and W4) preventing the damaging. The last two tests allowed to measure the lateral stiffness of the walls before to be tested again under cyclic loading (the results of the cyclic tests have not been processed yet).

It is worth to note that the horizontal force measured by the load cell is not the real force on the wall: it must be reduced for taking into account the friction force that rises between the trolley and the sliding plane at the base of the specimen. Hence the force experimented by the wall was equal to the force measured at the load cell reduced of the friction force. The friction coefficient was measured by moving the wall on the sliding surface before constraining the top.

Before starting the test every specimen was subjected to a vertical compressive force P of 80 kN approximately corresponding to a dimensionless axial force n=0.12, being n obtained as

$$n = \frac{P}{\sigma_0 bh} \tag{1}$$

in which b=740 mm is the width of the wall while h=210 mm is its thickness.

The value of the compressive force chosen for the tests is compatible with the condition in which a wall can be because of the service permanent and accidental weights.

3.2 Experimental results

The lateral force against the lateral displacement curves were determined (Fig. 5). These curves evidenced an homogeneous behaviour with a comparable ascending branch, with similar values of the lateral strength and with a comparable post peak branch.

Nevertheless a non homogeneous behaviour was observed by comparing the base cross-section moment against the variation of rotation evaluated in the first joint and the base cross-section moment against the mean curvature evaluated between the two cross-sections T and S including the first and the second joint (see Fig. 4) as it is going to be explained.

The moment M was evaluated taking into account the second order effects, that is

$$M = FL + P\delta \tag{2}$$

F being the horizontal reacting force experienced by the wall as a consequence of the horizontal displacement δ, and L being the height of the wall.

The curvatures were calculated as

$$\varphi = \frac{\varepsilon_2^I - \varepsilon_1^I}{H} = \frac{\varepsilon_2 - \varepsilon_1}{h} \tag{3}$$

ε_2^I and ε_1^I being respectively the averages of the strains evaluated on each side of the wall by means of the displacement transducers; H is the distance between the axes of the displacement transducers as shown in Figs. 4-c and 4-d, while ε_2 and ε_1 are the corresponding strains on the wall.

In Fig. 5-b the responses in terms of moments against mean curvatures interesting the part of the wall comprised between the cross-sec. S and the cross-sec. T, including the first and the second joint are depicted evidencing the different behaviour exhibited by the walls W1 and W2. The observation of these two specimens at the end of the tests evidenced, for the wall W1, the cracking of the joints at the base and of the nearest two joints and, for the wall W2, only the cracking of the joint at base as shown in Fig. 6. The curves depicted in Fig. 6-b, representing the moment against the variation of rotation evaluated in the first joint and the moment against the variation of rotation between the cross-sections T and S, clarify the phenomenon (note that the variation of rotation is simply indicated as “rotation” in the graph). For the wall W2, differently from the wall W1, the contribution of the first joint to the variation of rotation between the

cross-sections T and S was almost null evidencing that this joint did not crack. Further this variation of rotation was almost elastic. It evidenced that a much higher rotation had to be concentrated at the base of the wall being the sample W2 characterized by lateral displacements similar to that ones observed for the sample W1 (see Fig. 5-a). These circumstances are well represented by the Figs. 6-a and 6-c where the cracked joints are depicted (strong grey lines).

The behaviour of the sample W2 can be considered anomalous because similar to a rigid element differently from the sample W1 to which it was referred for the comparison with the model M-φ to be used for the prediction of the global response, as it is going to be explained.

It is worth to remark that the variation of rotation involving the first joint and the variation of rotation involving the cross-sections T and S can be obtained by multiplying the corresponding curvatures (Eq. 3) for the distance between the cross-sections with respect to the curvatures themselves are evaluated.

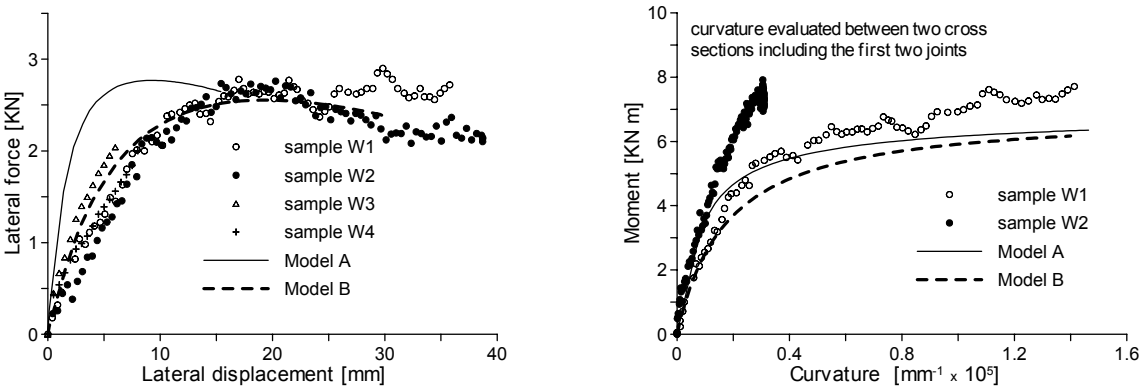

Figure 5 : Response of the walls: (a) lateral force against lateral displacement; (b) moment at the base cross-section against curvature evaluated between two cross sections including the first and the second joint.

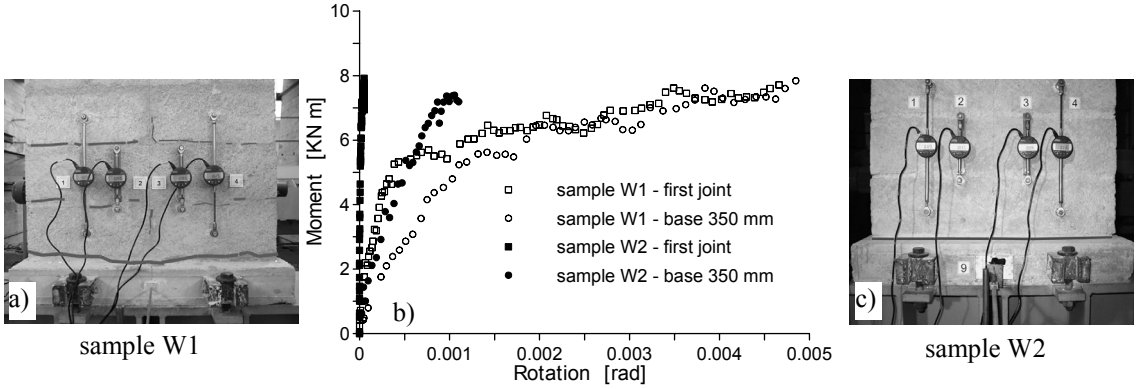

Figure 6 : Response of the walls: (a and c) distribution of the cracks at the base; (b) moments at the base cross-section against rotations.

In Fig. 5 the analytical responses predicted by means of the analytical model presented in this paper are also inserted. Their discussion is proposed in the next section.

4 ANALYTICAL RESPONSE

The wall was modelled by dividing the wall itself in elements characterized by a constant curvature. The moment-curvature law (M-φ) of the generic cross-section under a constant level of the normal force (P) was determined basing on the hypothesis of plane section and a constitutive σ–ε law obtained as explained in the second section. In this stage the weight of the wall was neglected producing a normal force much lower than the applied vertical force P.

The determination of the M-φ law was done by points verifying the equilibrium condition of the generic cross-section for each increment of the curvature φ.

Under the hypothesis of plane cross-section, the strain ε at the distance x from the neutral axis can be written as

$$\varepsilon = \varphi x \tag{4}$$

The translation equilibrium condition and the rotation equilibrium condition can be expressed as

$$P = \int_0^{x_c} \sigma(x) b dx\,, \quad P\frac{h}{2} - M = \int_0^{x_c} \sigma(x)(x_c - x) b dx \tag{5}$$

x_c being the distance of the neutral axis from the cross-section border line characterized by the maximum strain. By operating a change of variables in the integral functions appearing in Eq.(5) (from x to ε by means of Eq. (4)) Eq. (5) itself can be written in terms of ε_2 (that is the maximum strain in compression) and φ and can be specified for the cracked state and the uncracked state (see Cavaleri et al 2005).

By fixing a value of φ the two equilibrium equations allow the determination of the corresponding moment M. In this way the set of couples M-φ can be determined for the complete definition of the moment-curvature law characterizing the generic cross-section.

The moment-curvature response can be modelled in an optimal way by using the following dimensionless normalized analytical law

$$\tilde{m} = \frac{A_m \tilde{\varphi} + (D_m - 1)\tilde{\varphi}^2}{1 + (A_m - 2)\tilde{\varphi} + D_m \tilde{\varphi}^2}\,, \quad \tilde{m} = \frac{m}{m_0}\,, \quad \tilde{\varphi} = \frac{\varphi h / \varepsilon_0}{(\varphi h / \varepsilon_0)^*} \tag{6}$$

in which m is the dimensionless moment (m=M/$\sigma_0$bh^2) whose maximum value is m_0 and $(\varphi h / \varepsilon_0)^*$ is the value of the dimensionless normalized curvature associated to m_0. Referring to the M-φ curve obtained by the numerical procedure described above the value 0.0525 was obtained for m_0. By fixing this value of m_0 and by fixing A_m and D_m respectively equal to 55 and 0.5, Eq.(6) can be specialized. A comparison between the moment-curvature law numerically obtained by the using Eq. (4) and Eq. (5) and the moment-curvature law obtained by using Eq. (6) is shown in Fig. 7-a.

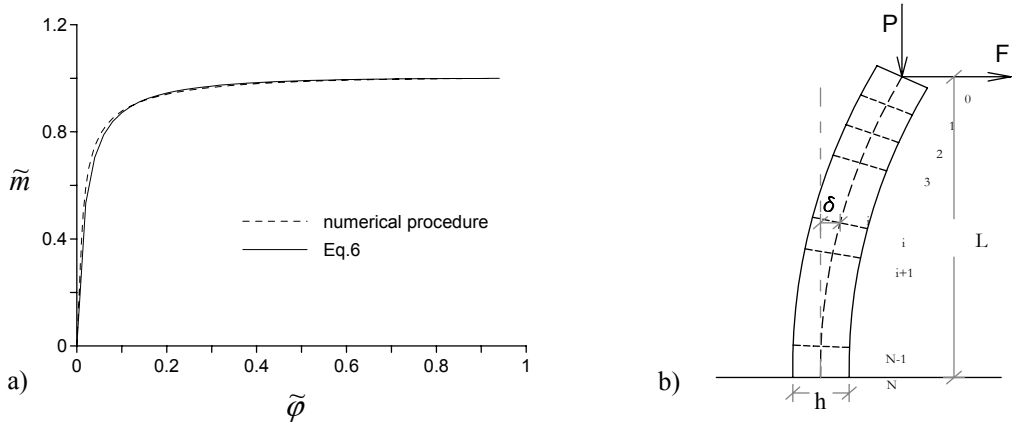

Figure 7: (a) Comparison between numerical and analytical moment-curvature law (b) and discretization of the wall for the evaluation of its global response.

The model obtainable by Eq. (6), specialized for A_m=55 and D_m=0.5, is also inserted in Fig. 5-b (model A) to be compared with the experimental response obtained for the wall between the cross-sections T and S including the first and the second joints: this part of wall can be considered representative of the mean behaviour of the masonry because it includes two half blocks, two joints and an entire block.

The analytical procedure for the evaluation of the response of the wall is based on the discretization of the wall itself in N elements characterized by the M-φ law before obtained.

The solution is obtained by writing the equilibrium equations and the compatibility equations

of each element and verifying them by means of a numerical procedure at each increment of the displacement at the top of the wall.

The result in terms of F-δ response obtained by using the M-φ law named model A is inserted in Fig. 5-a and evidences a slope of the ascending branch higher than that of the experimental curve. The disagreement with the experimental results is probably due to the not complete capability of the model to reproduce meanly the rotations that interest the cross-sections of the wall, in spite of the experimental curvatures and the analytical ones in Fig. 5-b, at least for the wall W1, do not seem so different. The cause may be the rotation of the base joint whose effect is probably do not taken into account by the above M-φ law. Alternatively or contemporary a scale effect not observed in the previous investigations (Cavaleri et al. 2005) may be.

A reduction of the parameters that define the analytical M-φ law (Eq. 6) allows a correction of the analytical results (model B in Fig. 5-b). In specific by fixing A_m=35 contrary to the value before fixed a good agreement between analytical and experimental results can be obtained in terms of F-δ curve. But the next step is to find a correlation between the reduction of the parameter A_m , the characteristics of the masonry, the boundary conditions and the level of the axial force interesting the wall.

REFERENCES

AlShebani, M.M. and Sinha, S.N. 2000. Cyclic compressive loading-unloading curves of brick masonry. *Structural Engineering and Mechanics* 9, p. 375-382.

Cantù, E. 1982. Axially loaded reinforced masonry walls under cyclic bending. *6th I.B.Ma.C., Sixth International Brick Masonry Conference, Rome,* p. 1043-1055.

Cavaleri, L., Failla, A., La Mendola, L. and Papia, M. 2005. Experimental and analytical response of masonry elements under eccentric vertical loads. *Engineering Structures* 27, p. 1175-1184.

Crook, R.N. 1982. The behaviour of concrete block masonry units under vertical loads. *Proceedings of Sixth International Brick Masonry Conference, Rome*, p. 627-638.

Drysdale, R.G. and Hamid, A.A. 1983. Capacity of concrete block masonry under eccentric compressive loading. *ACI Journal* 80, p. 102-108.

Griffith, M.C., Lam, T.K., Wilson, J.L. and Doherty K. 2004. Experimental investigation of the unreinforced brick masonry walls in flexure. *Journal of Structural Engineering* 130(3), p. 423-432.

Hansen, K.F. 2001. Uniaxial bending strength of masonry walls. *Masonry International* 14(3), p. 96-128.

Hatzinikolas, M., Longworth, J. and Warwaruk, J. 1980. Failure modes for eccentrically loaded concrete block masonry walls. *ACI Journal* 77, p. 258-263.

La Mendola, L. 1997. Influence of nonlinear constitutive law on masonry pier stability. *J. Structural Engineering, ASCE*, 123(10), p. 1303-1311.

La Mendola, L. and Papia, M. 2002. General stress-strain model for concrete or masonry response under uniaxial cyclic compression. *Structural Engineering and Mechanics Journal* 14(4), p. 435-454.

Lu, M., Schultz A.E. and Stolarski H.K. 2004. Analysis of the influence of tensile strength on the stability of eccentrically compressed slender unreinforced masonry walls under lateral loads. *Journal of Structural Engineering* 130(6), p. 921-933.

Macchi, G. 1982. Behaviour of masonry under cyclic actions and seismic design. *Proceedings of Sixth International Brick Masonry Conference, Rome*, p. 51-74.

Sargin, M. 1971. Stress-strain relationship for concrete and analysis of structural concrete sections. *Study N.4, Solid Mechanics Division, University of Waterloo,* M. Z. Cohn Ed.: Waterloo, Ontario.

Schultz, A.E., Ojard, N.J. and Stolarski, H. K. 2001. Critical axial loads for transversely loaded masonry walls. *Proceedings of 9th Canadian Masonry Symposium, New Brunswick, Canada*, (cd rom).

Yokel, F.Y. 1971. Stability and capacity of members with no tensile strength. *Journal of the Structural Division, ASCE*, 97, p. 1913-1926.